

# Assessment of Land Surface Temperature Variations and Implications of Land Use/Land Cover Changes: A Case of Malappuram Urban Agglomeration Region, Kerala, India

**Tania Viju**

Department of Architecture and Planning, National Institute of Technology, Calicut India

**Mohammed Firoz C and Sruthi Krishnan V**

Department of Architecture and Planning, National Institute of Technology, Calicut India

## ABSTRACT

Urbanization is taking place faster, and urban air temperatures are gradually rising in all cities across the world. Uncontrolled and unplanned urbanization leads to constant environmental threats and can alter local and regional climates. According to the survey published by Economist Intelligence Unit, in India, Kerala's Malappuram district ranks first among the fastest-growing urban areas globally, with a 44.05% growth rate. Hence, the present study aims to identify the hotspot regions of extreme heat within the Malappuram urban agglomeration region and suggest strategies for its improvement. The split-window algorithm retrieved land surface temperature (LST) for 1991, 1998, 2014, and 2020 using Landsat 5 ETM and Landsat 8 satellite imageries. A rising trend in LST has been detected in the last 30 years, and the mean value has increased by 1.70°C within the region. Among the selected hotspots, an LST increase of 1.84°C was observed for those areas with the highest increase in urban density with decreased vegetation. The increasing impact of urbanization and the subsequent change in land use patterns at the cost of greenery have caused a substantial effect on the local climate. Accordingly, planning and policy directions are proposed for the local government that can help provide awareness to the people through the effective implementation of mitigation measures.

## Article History

Received : 17 December 2022

Received in revised form : 24 June 2023

Accepted : 28 June 2023

Published Online : 31 August 2023

## Keywords:

Land Surface Temperature, Spatio-temporal analysis, Thermal hotspots, Urban Heat Stress, Urbanization

## Corresponding Author Contact:

firoz@nitc.ac.in

DOI: 10.11113/ijbes.v10.n3.1102

© 2023 Penerbit UTM Press. All rights reserved

## 1. Introduction

The impact of climate change has started drastically affecting our cities and settlements. Climate forecasts anticipate severe weather incidents to become more frequent and more intense. Hence, climate change thus becomes "the defining crisis of the time" (United Nations, 2020). Our cities and settlements are thus becoming risky places to live due to the increasing sea levels, harsh

weather, and rising temperatures (Appleton, 2021). The condition of heat stress will become more prevalent as a result of the increase in global temperatures brought on by climate change. Globally over 166,000 people died as a result of heatwaves between 1998 and 2017, including over 70,000 during the 2003 heatwave in Europe (World Health Organisation, 2022). On a worldwide basis, intense temperature occurrences are seen to increase in frequency, duration, and size. Between 2000 and 2016, there were over 125

million more persons exposed to heatwaves than there were in 2000 (World Health Organisation, 2022)). The 2022 heatwave across northwest India and southeast Pakistan has led to at least 90 deaths (Business Standard News, 2022). Population dependent on working outside to earn a living (such as street vendors, people working in farm and construction sites, traffic police, etc.) are particularly susceptible to intense heat because they typically lack access to cooling, which restricts their ability to deal with prolonged heat stress.

Land surface temperature (LST) is a fundamental metric for quantifying surface urban heat islands, calculating building energy use, and assessing heat-related concerns (Deng & Wu, 2013; Hu & Brunzell, 2013; Mathew et al., 2016; Weng & Fu, 2014). By modifying the land cover and energy balances, the shift in LST can affect surface air temperature, precipitation, and vegetation cover, which in turn has a significant impact on regional and worldwide environmental conservation (Wilson et al., 2003). Extreme weather events that happen frequently, the ongoing spread of desertification and the deterioration of flora, etc., pose a direct danger to regional ecological sustainability (Chen & Zhang, 2016). Therefore, researchers from all over the world have been interested in the study of LST as a significant quantitative parameter for ecological environment concerns (Feizizadeh et al., 2013; Haghighi et al., 2018; Madanian et al., 2018).

The rate of urbanization around the world is at an unprecedented peak. Planning professionals, environmentalists, and decision-makers all must address urbanization. Urban growth results in significant land use and land cover (LULC) changes (Rimal, 2012). According to Sterling & Duchame (2008), impermeable surfaces have largely replaced the naturally vegetated landscapes that once covered 40% of the Earth's surface with manmade land cover. These changes alter the properties of the land's surface, such as its thermal capacity, surface albedo, and soil moisture. While the temperature in the cities soars, the utilization of air conditioners increases. This in turn causes additional heat to be generated and makes it a vicious cycle. As a result, it will increase energy use, forcing generating stations to emit more harmful gases in order to satisfy the requirement. Increased pollution can result in poor environmental quality, which can cause a public health emergency. Hence rapid urbanization globally has caused a high risk to the quality of physical environmental elements.

As per a report by the United Nations, 55% of the global population resided in urban regions in 2018 compared to 30% in 1950 (United Nations, 2018). According to predictive calculations, the percentage will be around 68% by the year 2050, with developing nations having the greatest rate (United Nations, 2018). A major proportion of this urbanization, which will result in significant social, economic, and environmental changes, is expected to occur in Africa and Asia, according to the United Nations Population Fund (UNFPA). Rapid urban sprawl and land surface extension might be accelerated significantly by unchecked building construction and other economic activity, which would then trigger a serious environmental problem. Like the rest of the world, India is also rapidly urbanizing. A preliminary survey carried out by the Delhi-based Energy and Resource Institute (TERI) revealed that within just 15 years, the temperature in India's

megacities, namely Mumbai and Delhi, increased by 2°C to 3°C (Kikon et al., 2016). In Delhi National Capital Region, a study was conducted using data for the years 1998 to 2018 to determine the effect of altering land use patterns on the LST trend. It was found that the built-up area, which made up 21.4% of the total area in 1998, has expanded to 43.23% by 2018. While the vegetated surface declined from 11 percent to 7.40 percent by 2018. The urban sprawl development, rising urban population, deterioration of agricultural land, and vegetation cover have all been linked to a rise in LST and the development of thermal hotspots. Over the years, empirical comparison between LST and LULC has been suggested as a way to quantify the impacts of urbanization on regional climate (P. Singh et al., 2017; Tran et al., 2017; Zullo et al., 2019).

Kerala, a southern state of India, is also not different and has undergone significant demographic and economic profile changes in the past decades, which has resulted in this rapid urbanization (Banerji et al., 2014; Cyriac & Firoz C, 2022; Fathima Zehba et al., 2021; Kallingal & Mohammed Firoz, 2022) ("India is a federal constitutional republic governed under a parliamentary system consisting of 28 states and 8 union territories. All states have elected legislatures and governments. States are organised on a linguistic basis" (Sharma, 2007)). The recent urban growth rate of Kerala has become a challenge for the government and environmentalists (Praveen Lal & Nair, 2017; Sruthi Krishnan & Mohammed Firoz, 2020). Kerala's urban population growth rate exhibits a growing trend when compared to the global and national scenarios, where the rate is displaying a falling tendency (Cyriac & Firoz C, 2022). Compared to the decade before 2001, which had just 25.96% urban composition, the state's rate of urbanization increased to 47.72% in the year 2011 (Banerji et al., 2014; Cyriac & Firoz C, 2022; Kallingal & Joy, 2022; Kallingal & Mohammed Firoz, 2022; Sruthi Krishnan & Mohammed Firoz, 2020). The haphazard rise in urbanization has created significant changes in the state's land use and land cover. In the state, between 1985 and 2005, there was an increase in built-up land by 79%, a 7.65% decrease in forests and a decrease in fallow land by 23% (Browne, 2019). This might be the cause of the state's recurring flooding problems and other environmental risks (T.S. et al., 2022).

The present research focuses on identifying the hotspot regions of extreme heat within one of the upcoming urban agglomerations, namely Malappuram urban agglomeration in Kerala which ranks first among the fastest-growing urban areas globally (2015 – 2020) according to the survey published by the Economist Intelligence Unit. According to the census of 2011, the Malappuram urban agglomeration is the fourth-largest urban agglomeration in the state of Kerala and ranks 25 nationally among urban agglomerations in India. Malappuram is stated to have the highest growth rate of 13.45% among other districts in Kerala (Census of India, 2011). The high rate of urbanization and development in the study area leads to exploitation and overuse of environmental resources and creates an ecological imbalance that can have a negative impact on climate and lead to heat gain. Therefore, it is highly needed that a comprehensive assessment of the microclimate of a region to be done using LST variations to identify the hotspot regions of extreme heat and suggest suitable strategies and planning

recommendations. The planning for strategies is to be attempted as a multi-level, hierarchical process. The research area is selected as the anticipated urban area by 2030 based on the district's (administrative division of an Indian state) trend toward urbanization. Therefore, the study attempts to identify the thermal hotspot regions within the Malappuram urban agglomeration region in order to identify context-specific reasons for LST rise. This becomes the first-level assessment of the larger region which helps in deciding regions in order to perform a detailed assessment at the LSG level (Local Self Government is the third level of the government below the state level that manages the local affairs) in subsequent second and third-level assessments for proposals and policy recommendations. The research also attempts to propose a framework of strategies to be taken up at each planning level. By adopting a multi-level, hierarchical process for planning strategies, organizations can foster coordination, integration, flexibility, and effective decision-making. It ensures that strategies are aligned, resources are optimized, and objectives are integrated across different levels, leading to a more coherent and successful implementation of strategic initiatives.

Accordingly, the present study is organized into six sections, which begin with an introduction. Following this, section two details the literature review on strategies for mitigating heat gain. The third section elaborates on the methodology followed in order to arrive at the research objective. Thermal hotspots are identified in section 4 and spatio-temporal analysis of LST, NDVI and Google Earth images are performed to assess the effects of changing land use and other factors. The fifth section discusses various case-specific and hierarchical planning recommendations to mitigate the effect and the final section concludes the research.

## 2. Literature Review

Several LST studies have been conducted in India's developed and developing cities. The main causes of the increased temperature, according to most of this research, are due to changes in land-use patterns and increased urban density as mentioned in the introduction section.

As urbanization is seen as a never-ending process, it is increasingly important to take the measures required to achieve a fine balance between the environment and urban expansion. Based on the works already carried out by previous researchers, the mitigation strategies can be classified into 6 heads - vegetation, water bodies and features, materials and shading, urban geometry, transport and energy (Ruefenacht & Acero, 2017). Various tree planting strategies within the urban areas, with local, micro and macro scale forestry and green parks are to be looked into to combat the reduction in vegetation cover as they would help in increasing the rate of evapotranspiration (Norton et al., 2013). Also, green roofs, green pavements, and vertical greenery can be taken up. It results in significant reductions in the amount of energy usage as it reduces the dependency on cooling appliances. Infrastructure greenery on transportation routes can be given, where existing infrastructure, such as tunnels, bridges, motorways, and bus stops, can be enhanced by vegetation to reduce the impact of dark pavements on heat gain.

The coverage of the shaded areas along with the wind condition is influenced by building layout, the placement of urban features, building proportion and orientation. Additionally, sufficient urban planning is essential at a coarser spatial scale to take advantage of the regional environment and airflow, create appropriate wind paths that access the urban area, and eliminate the building up of heat. For example, varying building heights, urban elements that guide wind flow, mixed land use, wider streets, etc can reduce the trapping of heat.

Water bodies and features are beneficial in hot and dry surroundings, but the effects are less in humid areas due to the higher levels of water vapour present in the air, hence it cannot additionally cool the environment. Water's heat capacity allows it to absorb thermal energy from incoming solar radiation. Increasing surface reflectivity is another mitigation approach. As a result, high albedo building materials should be utilized and cool roofs, cool pavements, etc. can be adopted as they will store less heat and maintain a low temperature. Encouragement of the use of public transport and active mobility should be carried out. The use of renewable energy sources and heat recovery systems should be encouraged, and low-carbon fuels should be promoted.

According to a comparative analysis of the two Indian megacities, Mumbai has a greater proportion of heat gain than Delhi (Singh et al., 2014). The research implies that Delhi encountered lower intensity compared to Mumbai because of the city's mixed land use, the presence of green belt throughout the roads, the Delhi Ridge forests, also the Yamuna River, all of that have an impact on and result in a drop in LST (Grover & Singh, 2016). While in the case of Mumbai, the reduced vegetation and diminished carrying capacity of Mumbai's river have contributed to an increase in LST. This causes the heat to become retained in the inhabited areas, creating a significant Urban Heat Island (UHI) effect (Sannigrahi et al., 2017).

## 3. Materials and Methods

### 3.1 Study Area

Malappuram, located in Kerala, India, is one of the state's 14 districts and is characterized by its proximity to the Nilgiris Hills in the east and the Arabian Sea in the west. It holds the distinction of being Kerala's most populous district, accommodating roughly 13% of the state's total population (Census of India, 2011). A rapid transformation in the workforce composition from agriculture to non-agriculture has been observed when comparing the census data from 2001 and 2011. According to the survey published by Economist Intelligence Unit, Kerala's Malappuram district ranks first among the fastest-growing urban areas globally (Nijeesh, 2020). The urban population in Malappuram was only 300,000 in 2001, and it increased to 16,00,000 in 2011, an increase of more than five folds in a decade. (Nijeesh, 2020). This exponential growth reflects the rapid pace of urbanization in the district, leading to the selection of the urban agglomeration region as the focus of the study. (Figure 1). The region is delineated considering the present and future urban trends likely to be followed by the region and the anticipated urban area of 2030.

The climate in the study area is generally hot and humid. Relative humidity ranges from 84 to 94 percent during morning hours (Sreenath, 2013). Kerala has been experiencing a scorching summer, with daytime temperatures in several parts of the state reaching above 37°C in 2019. Kerala lost 3 lives in the same year,

and 125 people were given medical help due to increasing temperatures (*The Hindu*, 2019). Two places in Malappuram were among the top 8 places within Kerala in maximum temperature observed - Wandoor with 40.30°C and Chugathana with 39.40°C (*Skymet Weather Services*, 2019).

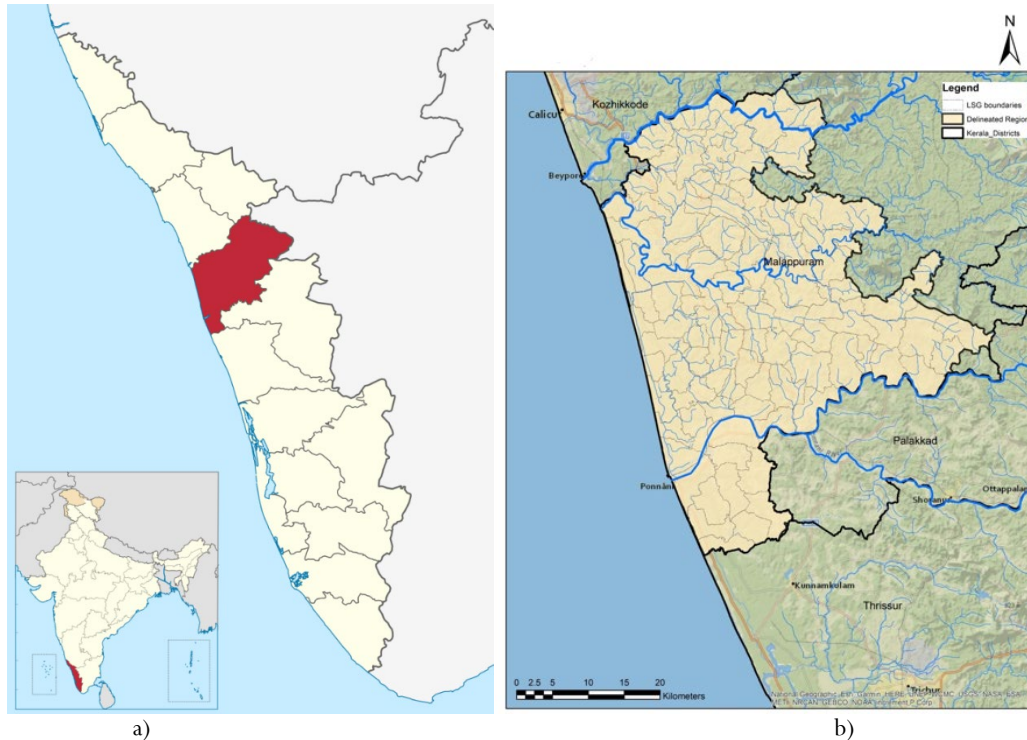


**Figure 1** Map of a) Kerala, India b) study area (Malappuram urban agglomeration)

### 3.2 Tools and Techniques

The LST can be measured at different scales using various methods. City level or a larger scale can be measured using thermal remote sensing satellite data as it has got extensive spatial coverage. Temporal coverage and spatial resolution are limited and it is impacted by weather and atmosphere. The neighbourhood scale assessment can be carried out using an aircraft/ thermal scanner which will be having better resolution but higher costs and irregular coverage. Spatial resolution depends on the sensor and aircraft altitude. At the street scale using ground-based techniques, an infrared thermometer can be utilized, which doesn't require any atmospheric corrections. It helps to provide a unique perspective of urban features with high temporal resolution (Voogt & Oke, 2003). According to Cheval & Dumitrescu (2009), satellite temperature data yield more accurate results than interpolated ground station values. The present study is carried out using satellite imagery as it covers a large area and this will help in the broader scale or first level of assessment which can aid in deciding areas that require further studies.

Assessment using satellite imagery includes three popular retrieval methods - single-channel, split-window and multi-angle techniques. The most often used method for retrieving LST from

thermal emission in the infrared or microwave range using remote sensing data is the split-window technique because the accuracy of predicted LST using two thermal bands is higher than that of a single band. Only this technique is exempted from accurate atmospheric temperature/water vapour content measurements compared to other LST acquisition techniques. It is vital to keep in mind that inaccuracies in the outcomes will be caused by uncertainties in the atmospheric profile when using the single-channel and multi-angle approaches to retrieve emissivity and LST (Sattari & Hashim, 2014). Hence for the current study, the split window algorithm will be utilized.

### 3.3 Data sources

Remote sensing data is mainly used in the present study. The data was collected from the United States Geological Survey (USGS) website (United States Geological Survey, 2022). Accordingly, 8 Landsat imageries from 1991 to 2020 were acquired because they best represent the urbanization, change in vegetation and the possible heat gain process. The period is so taken as in Kerala the urbanization pattern was seen to have a normal rate during 1990 to 2000 and it started increasing exponentially after 2011. For 1991 and 1998, Landsat 5 TM (spatial resolution 120m resampled to 30m) are used, while for 2014 and 2020, Landsat 8 (spatial resolution 100m resampled to 30m) imageries are taken. Two

imageries were required for each year as the study area fell into two different tiles. Higher mean maximum temperatures are observed in the months of March and April (34°C) (Figure 2).

Also due to the issues of continuous data availability and cloud coverage, the month of March is chosen, as a closer acquisition date considering the temporal data was better available for that month (Table 1).

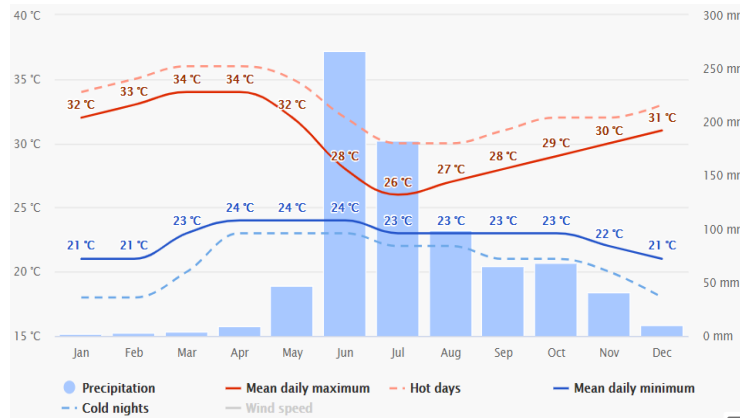


**Figure 2** Mean maximum temperature of Malappuram district in 2022 (Source: Meteoblue)

**Table 1** Metadata of used satellite imageries (Source: (United States Geological Survey, 2022))

Sensor	Path	Row	Date of acquisition
Landsat 5 (TM)	144	52	12 March 1991
Landsat 5 (TM)	145	52	03 March 1991
Landsat 5 (TM)	144	52	14 March 1998
Landsat 5 (TM)	145	52	10 March 1998
Landsat 8	144	52	11 March 2014
Landsat 8	145	52	02 March 2014
Landsat 8	144	52	12 March 2020
Landsat 8	145	52	19 March 2020

LULC maps were acquired from ‘Bhuvan’, a geo-platform of the Indian Space Research Organisation (ISRO). The LULC maps were created using multi-temporal satellite data from Resourcesat-2 LISS III (spatial resolution - 30 x 30 m) for the years 2005-06, 2010-11, and 2015-16 as shown in Figure 3. A hybrid technique (Decision Tree - See5, Supervised Maximum Likelihood Classifier) was used to classify the satellite data. (National Remote Sensing Agency, 2007).

### 3.4 Methodology

The overall methodology followed in the research is given in Figure 4. From the background study conducted, the study area is selected, followed by the acquisition of corresponding satellite imageries. LST and Normalized Difference Vegetative Index (NDVI) retrieval algorithms are reviewed in the coming sections. The study area is mapped and, LST and NDVI estimation and analysis are carried out. Pearson's correlation analysis is used to verify the relations between LST and NDVI. Based on the remote sensing observations, thermal hotspot regions are identified and spatiotemporal variations within the region are analyzed with the help of LST, NDVI and Google Earth images to understand the impact of change in land use. Finally, suitable mitigation strategies are proposed.

#### 3.4.1 Retrieval of LST and NDVI

The split-window algorithm was employed to calculate the surface temperature. Digital Number (DN) values were converted to spectral reflectance and later converted to brightness temperature. For Landsat 8, emissivity correction is also required to accurately calculate the LST. It is carried out using NDVI calculations as shown in Figure 4. Bands 4 and 5 were used to retrieve NDVI, followed by the calculation of the proportion of vegetation which helps in the determination of ground emissivity. The detailed procedure to retrieve LST and NDVI of the study area is explained as follows:

- i. Conversion of DN to Top of Atmosphere (TOA) spectral radiance ( $L_{\lambda}$ )

Conversion of the DN data into spectral radiance was carried out using band 6 from Landsat 5 ETM and band 10 from Landsat 8. It was calculated based on the following equations (Aik et al., 2020; Avdan & Jovanovska, 2016; Sholihah & Shibata, 2019) expressed as Eq. (3.1) and Eq. (3.2):

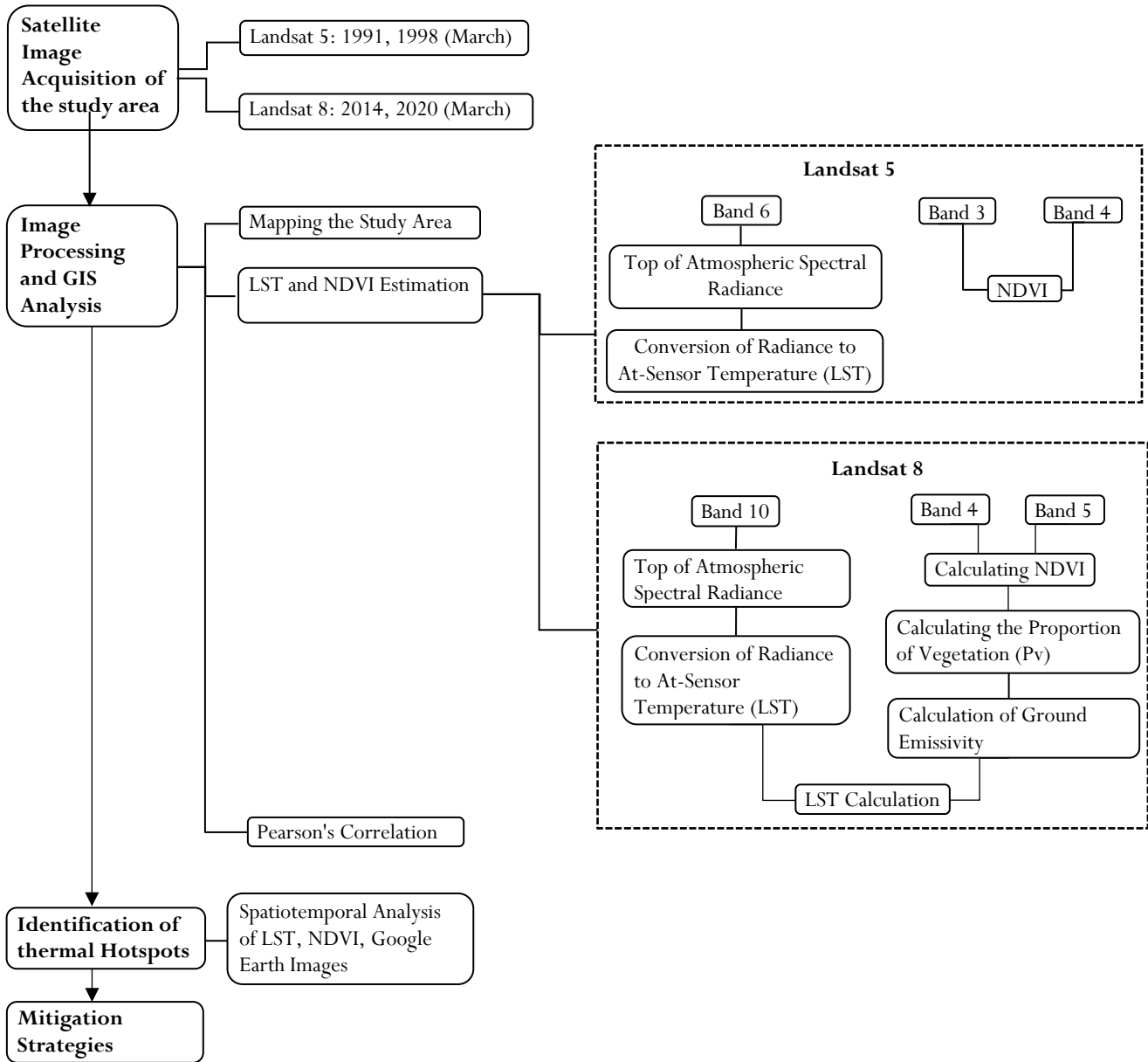


Figure 3 Methodology of the study

a) For Landsat 5 ETM

$$L_{\lambda} = \frac{L_{MAX} - L_{MIN}}{Q_{CALMAX} - Q_{CALMIN}} \times (Q_{CAL} - Q_{CALMIN}) + L_{MIN} \quad (3.1)$$

Where (Aik et al., 2020),

$L_{\lambda}$  = Cell value as radiance

$L_{MAX}$  = Spectral radiance scales to  $Q_{CALMAX}$

$L_{MIN}$  = Spectral radiance scales to  $Q_{CALMIN}$

$Q_{CAL}$  = Digital Number

$Q_{CALMAX}$  = Maximum quantized calibrated pixel value (typically 255)

$Q_{CALMIN}$  = Minimum quantized calibrated pixel value (typically 1)

b) For Landsat 8

$$L_{\lambda} = M_L Q_{Cal} + A_L \quad (3.2)$$

Where (Sholihah & Shibata, 2019),

$M_L$  = Band-specific multiplicative rescaling factor (for band 10 or 11 = 3.3420E-04)

$A_L$  = Band-specific additive rescaling factor (for band 10 or 11 = 0.10)

$Q_{cal}$  = Digital Number.

$L_{\lambda}$  = TOA spectral radiance (Watts/ (m<sup>2</sup> × srad × μm))

The above-mentioned data is available in the meta-data document of the satellite image data

- ii. Conversion of TOA spectral radiance ( $L_{\lambda}$ ) to TOA brightness temperature (Celsius)

$$BT = \frac{K_2}{\ln\left(\frac{K_1}{L_{\lambda}}\right) + 1} - 273.15 \quad (3.3)$$

Where (Aik et al., 2020),

BT = TOA brightness temperature (°C)

$L_{\lambda}$  = TOA spectral radiance

$K_1, K_2$  = band-specific thermal conversion constants (Table 2)

**Table 2** Landsat thermal conversion constant (metadata) (Source: USGS Earth Explorer, 2022)

Sensor	Band	$K_1$ : W/(m <sup>2</sup> .sr.mm)	$K_2$ : Kelvin
Landsat 5	6	607.76	1260.56
Landsat 8	10	774.8853	1321.0789
Landsat 8	11	480.8883	1201.1442

- iii. Emissivity Correction using NDVI Method

Emissivity must be included in the calculation of LST, using the near-infrared and visible bands, even though it is feasible to evaluate radiance and temperature data without it (Aik et al., 2020; Avdan & Jovanovska, 2016; Carlson & Ripley, 1997; Estoque & Murayama, 2017; Gazi et al., 2021; Gohain et al., 2021; Kafy et al., 2021; Sekertekin & Bonafoni, 2020; Sobrino et al., 2004; Twumasi et al., 2021).

- iv. Calculate the NDVI:

For NDVI calculations (Eq.(3.4)), Landsat visible (Band 4) and near-infrared bands (Band 5) were used (Estoque & Murayama, 2017).

$$NDVI = \frac{Band\ 5 - Band\ 4}{Band\ 5 + Band\ 4} \quad (3.4)$$

- v. Calculate the proportion of vegetation  $P_v$  (Carlson & Ripley, 1997; Sekertekin & Bonafoni, 2020).

$$P_v = \left(\frac{NDVI - NDVI_{min}}{NDVI_{max} - NDVI_{min}}\right)^2 \quad (3.5)$$

The minimum and maximum values of NDVI calculation performed in the preceding step are designated as  $NDVI_{min}$  and  $NDVI_{max}$  (Eq. (3.5)).

- vi. Calculate Emissivity  $\epsilon$ :

The effectiveness of conveying heat energy from the surface into the atmosphere is measured by the land surface emissivity, which

is a proportionality factor that scales blackbody radiance (Planck's law) to forecast emitted radiance (Sobrino et al., 2004; Twumasi et al., 2021).

$$\epsilon = 0.004 * P_v + 0.986 \quad (3.6)$$

- vii. Calculate the Land Surface Temperature:

Emissivity-corrected LST is calculated as shown below (Estoque & Murayama, 2017):

$$LST = \frac{BT}{1 + \left(0.00115 * \frac{BT}{1.4388}\right) * \ln(\epsilon)} \quad (3.7)$$

#### 4. Results and Discussions

The spatial distribution of LST and LULC for the Malappuram district is depicted in Figure 5 and Figure 6. Temperature is seen to increase towards the southwest side, as shown in Figure 5, which is the delineated region. The majority of the study area has a maximum temperature range of 32°C - 34°C. On comparing the LST map with that of the LULC map (Figure 6) of the same year, it can be seen that less amount of vegetation, and the increased built-up area in the study region, could be the reason for the increased temperature when compared to the surrounding regions (Esri, 2020).

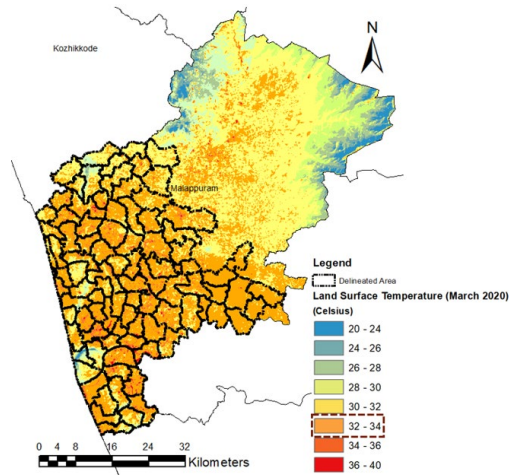


Figure 4 LST Map – March 2020

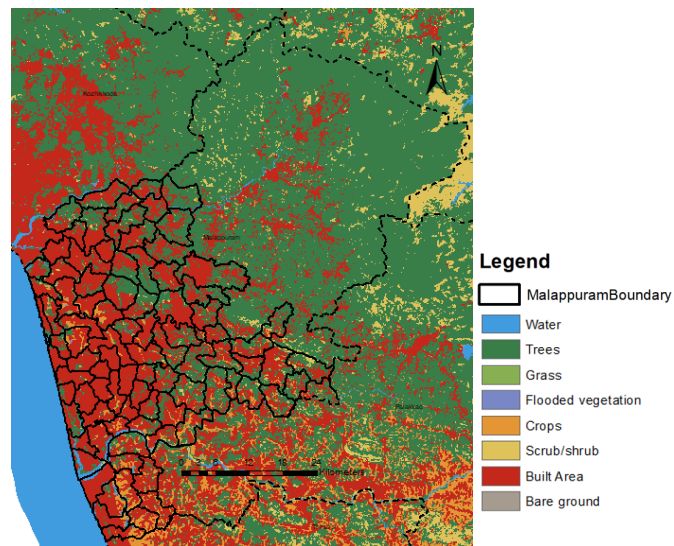
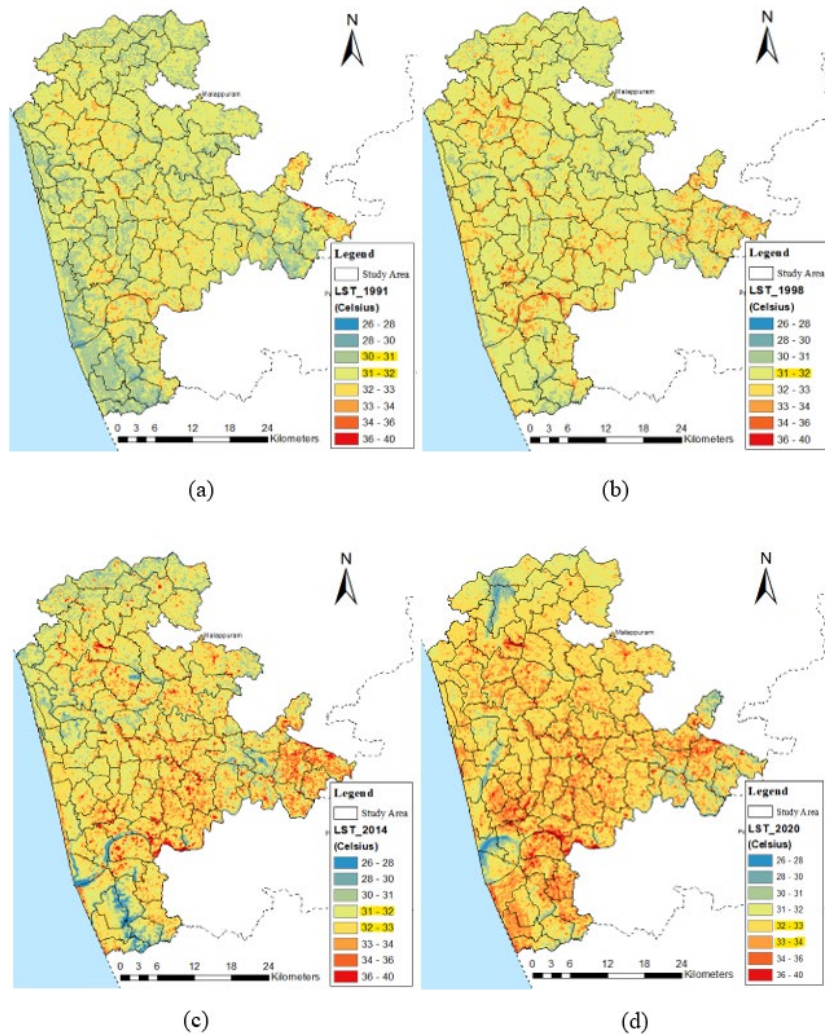


Figure 5 LULC map of 2020 (Source: Esri)

#### 4.1. Spatiotemporal Analysis of Land Surface Temperature

From the spatiotemporal analysis (Figure 7), it is observed that in 1991 the temperature ranged from 30°C - 32°C with the mean value being 31.66°C, while in 1998, the majority region had a

temperature range of 31°C – 32°C with 31.78°C as the mean. In 2014, it increased to 31°C – 33°C with a mean value of 32.56°C, and currently, in the case of 2020, the range has increased to 32°C – 34°C having a mean of 33.36°C. Hence, we can infer that around 1.70°C rise is seen over 30 years time period. Site-specific reasons will be analyzed in the following sections.



**Figure 6** LST map (a) 1991 (b) 1998 (c) 2014 (d) 2020

The temperature rise that has been recorded between 1991 and 2020 is consistent with the prediction by the Intergovernmental Panel on Climate Change (IPCC) in its Fifth Assessment Report (AR5), an organization based in Geneva, Switzerland (*The IPCC Fifth Assessment Report*, 2014). As stated in the report, the rise in global average temperature by the century's end is to be between 2.6 and 4.8 °C. This is mostly due to urbanization and the cities' emission of gases that intensify the greenhouse effect (Kaiser et al., 2022; Revi et al., 2014; Rosenzweig et al., 2018). The contribution of the increasing urbanization rate in the district as mentioned in the Introduction section to the temperature gain is evident in this study.

#### 4.2 Spatiotemporal Analysis of Normalized Difference Vegetative Index

NDVI is used to measure the greenness of vegetation and is useful for determining vegetation density and detecting changes in plant health. Values close to 0, as well as negative values, represent water bodies, 0 to 0.2 represent built-up and barren land, and +1 represents the highest possible vegetation (Guha & Govil, 2020).

From the LULC map shown in Figure 9, a considerable increase in built-up area with decreased vegetation is observed. Hence the impact of decreased vegetation on the LST increase was analyzed. On analysis from 1991 to 2020 (Figure 8), the maximum value decreased from 0.90 to 0.60, which indicates that the vegetation intensity is decreasing. Also, the spatial extent of the green region can be seen to be decreasing over the years, with more areas of lesser intensity vegetation in the case of 2020 and it is quantitatively validated as shown in Table 3. Cross-referencing with Figure 6 shows the spatial correlation between LST and NDVI. It can be interpreted that low LST areas either have the highest NDVI values indicating high vegetative areas or less than 0 NDVI values indicating the water bodies. This is validated through the statistical correlation carried out in the next section. Also, it is observed that over the years, the increase in LST values spatially aligns with the increase in lower NDVI values. The increase in lower NDVI values indicates the change in land use to more of built-up regions. Detailed site-specific interpretations are carried out in Section 4.1.5.

Table 3 NDVI Temporal Variation

NDVI	Area								% Change from 1991 to 2020
	1991		1998		2014		2020		
	Pixel count	%							
VERY LOW	75728	3.97	81090	4.25	41560	2.18	40081	2.10	-1.87
LOW	190404	9.98	204505	10.72	233812	12.26	268297	14.07	4.08
MEDIUM	190224	9.97	227069	11.91	559997	29.36	623023	32.67	22.69
HIGH	363405	19.05	444223	23.29	863830	45.29	780166	40.91	21.85
VERY HIGH	1087475	57.02	950349	49.83	208037	10.91	195669	10.26	-46.76

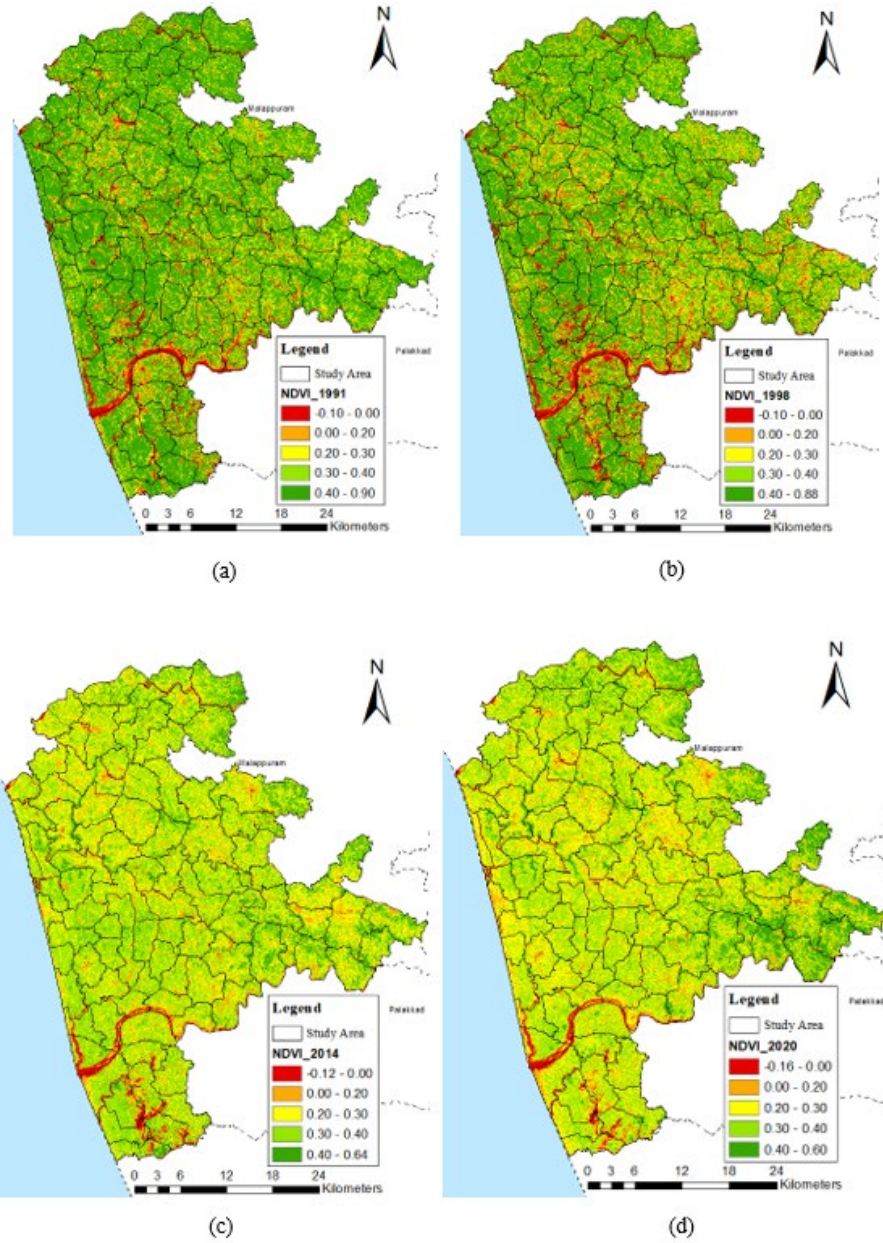


Figure 7 NDVI map (a) 1991 (b) 1998 (c) 2014 (d) 2020

### 4.3 Statistical Analysis

To validate the relationship between LST and NDVI, statistical analysis was performed using the Pearson correlation coefficient matrix. A sample size of 1048 paired observations was taken and the Pearson Correlation coefficient ( $r$ ) is obtained to be 0.41. The p-value of this correlation is  $1.33E-43$ , which is less than the significance level (0.05) indicating a statistically significant correlation. Also, the results of the LST-NDVI correlation scatter plot (Figure 8) reveal a negative relationship, with locations with

high NDVI values having low temperatures than regions with low NDVI values, which validates the spatial interpretation. The reason can be that plants are excellent absorbers. Flora and moisture-holding soils use a substantial quantity of absorbed radiation during evapotranspiration and produce water vapor, which helps to cool the air in their proximity and therefore reduces the temperature (Kikon et al., 2016). Also, a few values with less than 0 NDVI are seen to have low LST, which is the water bodies having a low-temperature effect.

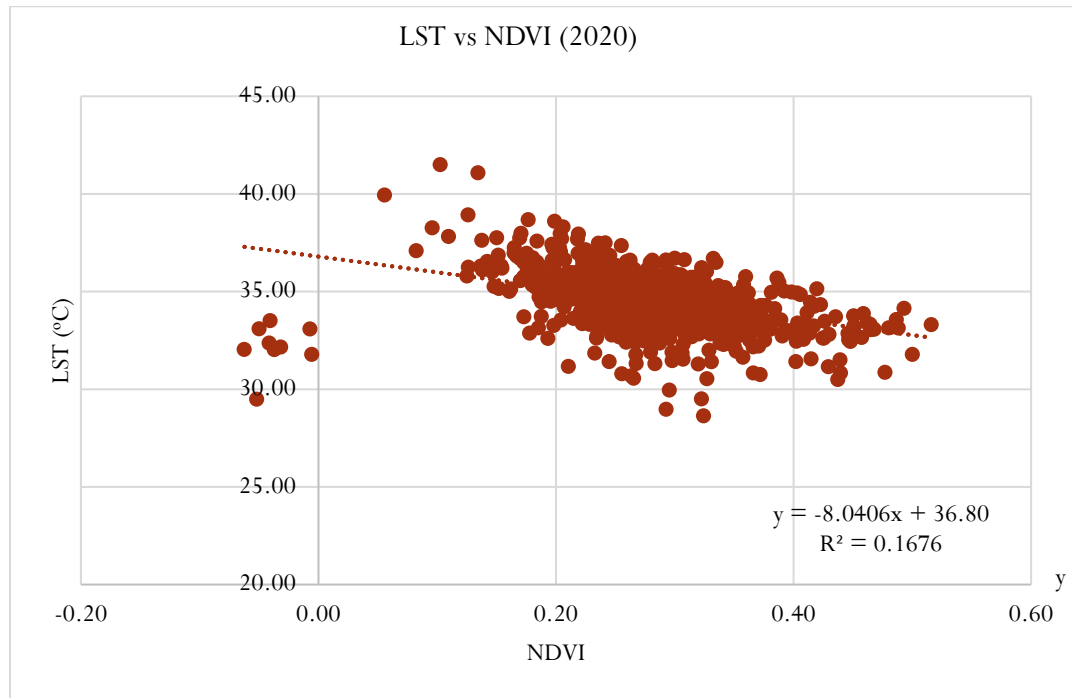


Figure 8 Correlation Analysis - LST vs NDV

I

### 4.4 Spatiotemporal Analysis of LULC Change

The LULC change analyses of the years 2005–06, 2010–11, and 2015–16 were performed for the categories of built-up, agricultural, forest, wetland/water bodies, and barren/uncultivable land in the 1727 sq. km. of Malappuram urban agglomeration region. While analyzing the percentage difference in the area over the years for different land covers, the built-up area has significantly increased over the years, which can be related mostly to the conversion of cultivable land as shown in Table 4. It is seen that built-up land use has increased by 5.73%

inclusive of the urban, rural and industrial land uses (by 98.95 km<sup>2</sup>) between 2005-2010 and 4.86% (84.01 km<sup>2</sup>) between 2010-2015 leading to an overall increase of 182.96 km<sup>2</sup>. Subsequently, the decrease in agricultural land is seen to be about 156.32 km<sup>2</sup> of area. The significant change in built-up land use has been for rural areas due to the transition from agricultural land to rural built-up. It may lead to new town centers and higher urbanization in the future and lead to more rise in LST. The encroachment and degradation of wetlands for agricultural uses have led to a slight drop in water bodies and wetlands in the region of study. These all can be attributed as reasons for the increased temperature and other concerns seen over the years.

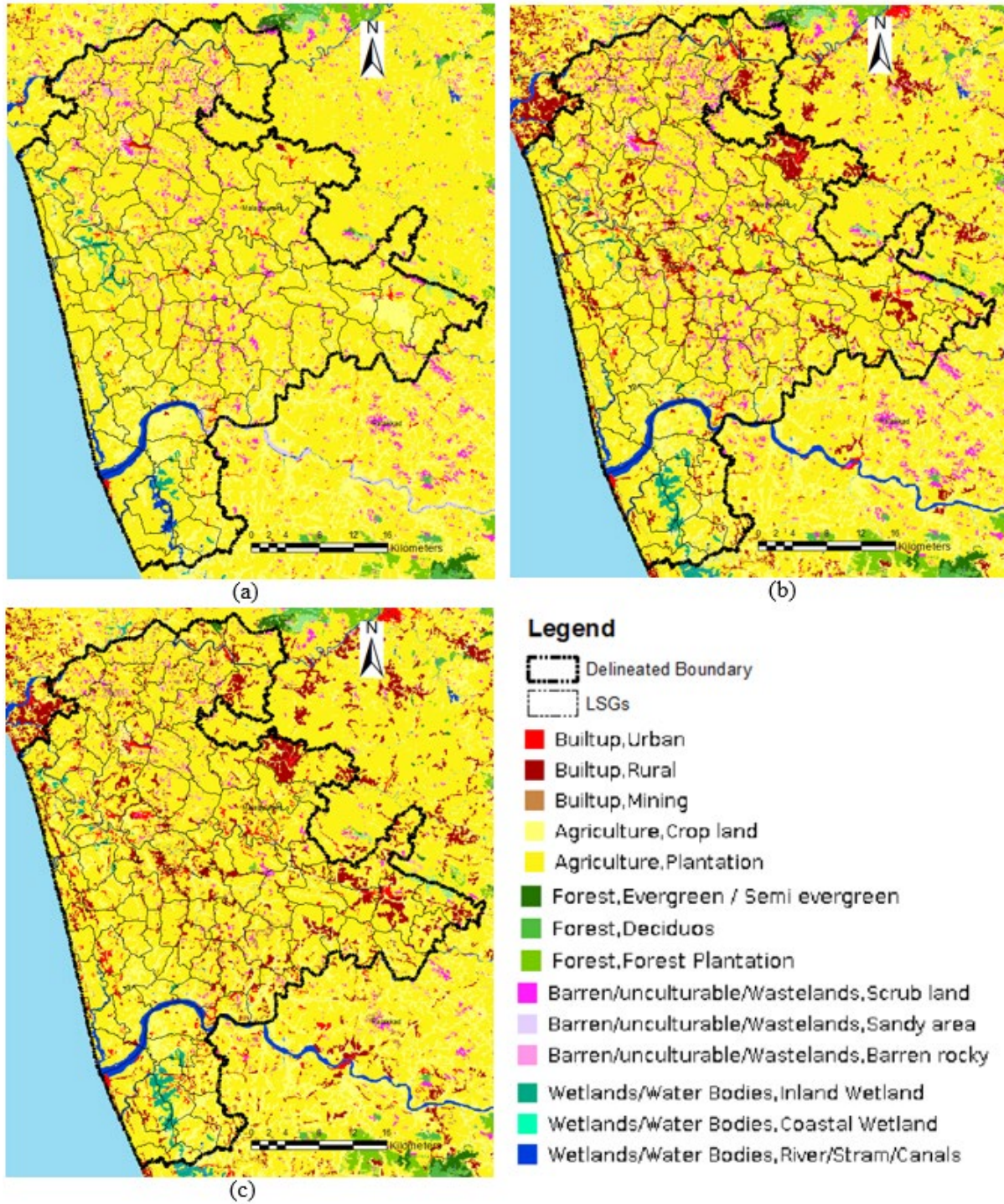


Figure 9 LULC map (a) 2005-06 (b) 2010-11 (c) 2015-16 (Source: Bhuvan WMS overlay)

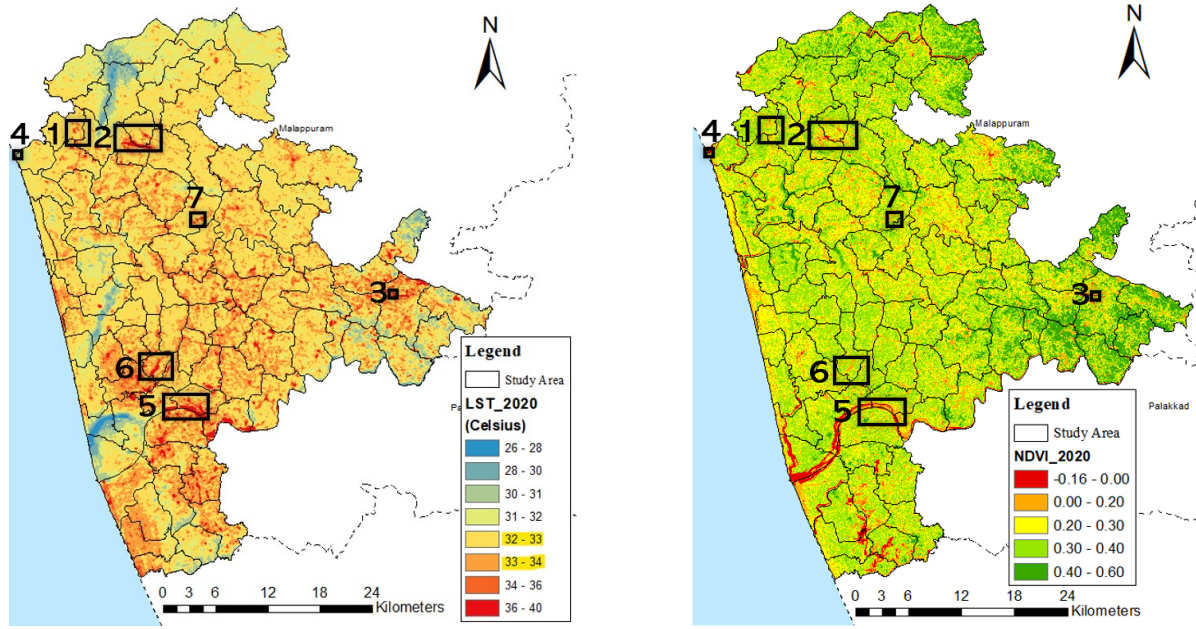
**Table 4** LULC Temporal Change (Source: Extracted from (Bhuvan, 2021))

LAND USE			AREA (km <sup>2</sup> )			% DIFFERENCE
L1	L2		2005	2010	2015	2005-2015
<b>Built-Up</b>	Urban	Compact	14.33	14.39	5.99	<b>+10.60</b>
		Sparse			32.62	
	Rural		18.19	117.08	172.72	
	Industrial				4.15	
	<b>Total</b>		<b>32.52</b>	<b>131.47</b>	<b>215.48</b>	
	<b>% Area Covered</b>		<b>1.88</b>	<b>7.61</b>	<b>12.48</b>	
<b>Agriculture</b>	Plantation		1314.72	1257.06	1209.30	<b>-9.06</b>
	Cropland		220.38	179.26	169.49	
	<b>Total</b>		<b>1535.10</b>	<b>1436.32</b>	<b>1378.78</b>	
	<b>% Area Covered</b>		<b>88.90</b>	<b>83.18</b>	<b>79.84</b>	
<b>Forest</b>	Evergreen Broadleaf		1.39	1.36	1.34	<b>-0.01</b>
	Deciduous Needleleaf		0.16	0.16	0.16	
	Mixed Forest		1.04	1.02	0.98	
	<b>Total</b>		<b>2.59</b>	<b>2.54</b>	<b>2.48</b>	
	<b>% Area Covered</b>		<b>0.15</b>	<b>0.15</b>	<b>0.14</b>	
<b>Wetlands/ Waterbodies</b>	Wetlands		24.14	19.43	18.94	<b>-0.07</b>
	Waterbodies		55.20	55.07	54.34	
	<b>Total</b>		<b>79.34</b>	<b>74.5</b>	<b>73.28</b>	
	<b>% Area Covered</b>		<b>4.59</b>	<b>4.31</b>	<b>4.24</b>	
<b>Barren/ Uncultivable/ Wastelands</b>	Barren land		3.83	2.22	1.32	<b>-1.19</b>
	Scrubland		73.48	68.58	38.44	
	Wastelands				0.22	
	Mining/ Quarrying			11.23	16.87	
	<b>Total</b>		<b>77.31</b>	<b>82.03</b>	<b>56.84</b>	
	<b>% Area Covered</b>		<b>4.48</b>	<b>4.75</b>	<b>3.29</b>	

Each land use land cover has got varied reflectance properties and has got a substantial influence on LST. The shift from vegetation cover and water bodies to built-up land can impact LST as they alter the roughness and surface reflectance properties due to the use of anthropogenic substances, multi-story structures, asphalt, and concrete for urban development. The areas of high temperature are depicted in the shades of orange and red and correspond to built-up areas, barren or fallow land, dried river beds, etc. whereas the cooler areas are mapped by the shades of yellow and blue and correspond to the forest, agricultural land, wetlands and water bodies, as shown in Figure 6(d). Location-specific reasons will be examined in the next section. This analysis has shown how LULC modifications can be used as one of the broad factors among others to monitor changes in urban climate.

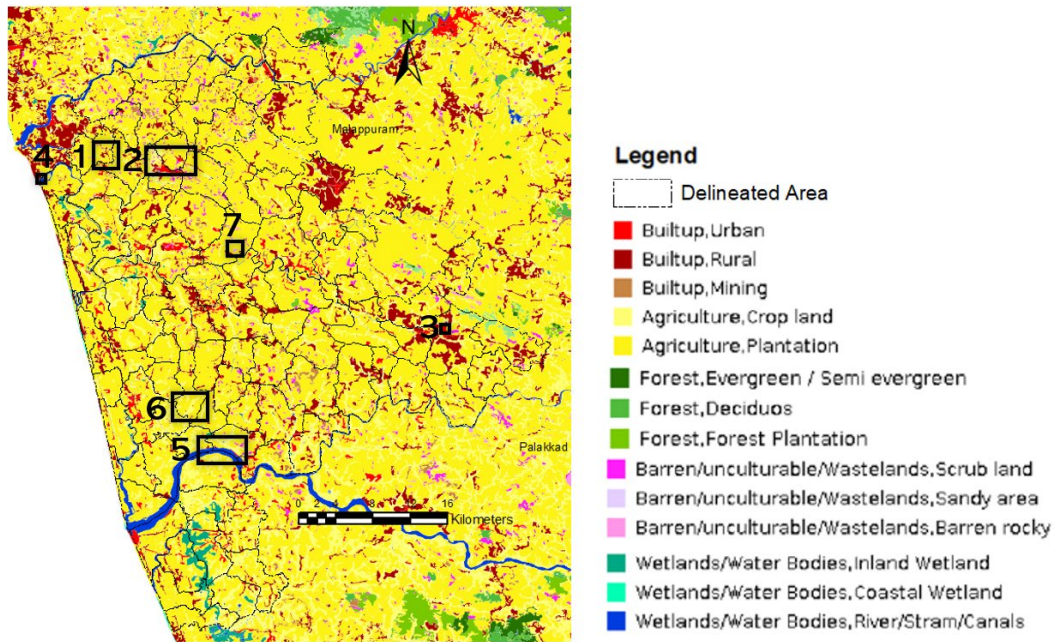
#### 4.5 Thermal Hotspots

Based on the remote sensing observations, thermal hotspot regions are identified and spatiotemporal variations within the region are analyzed and quantified with the help of LST, NDVI and Google Earth images to understand the impact of change in land use as depicted in Table 5. Hotspot areas are marked from 1 to 7 as shown in Figure 10 namely 1) KINFRA industrial area (Kerala Industrial Infrastructure Development Corporation is a government agency to promote industrialization in the state); 2) Calicut International Airport (located at Karipur, Malappuram district opened on 13 April 1988) and Kondotty region; 3) Perintalmanna built-up area; 4) Kadalundi bird sanctuary area; 5) Bharathapuzha River, 6) fallow land and finally 7) barren land'.



(a)

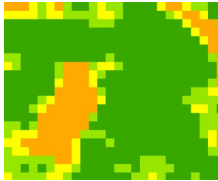
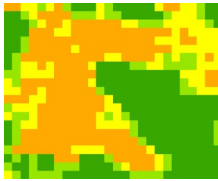
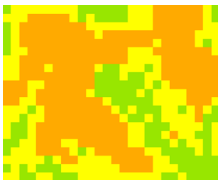
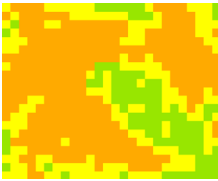
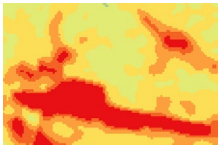
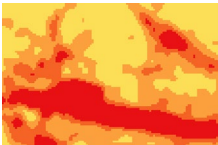
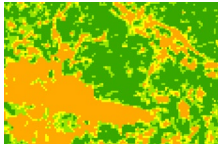
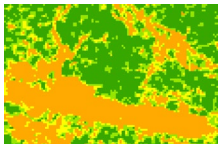
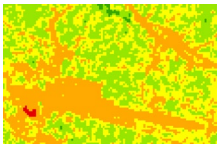
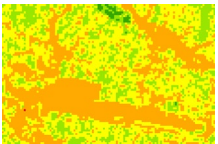
(b)

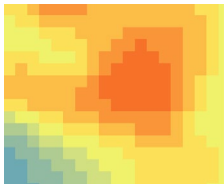
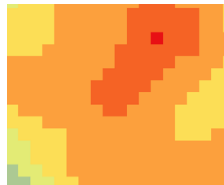
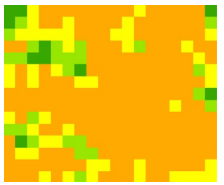
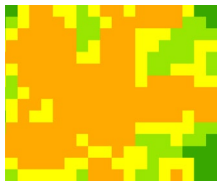
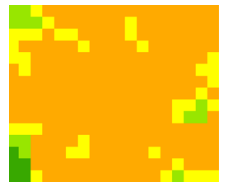
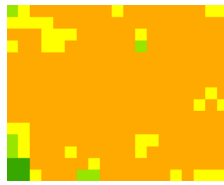
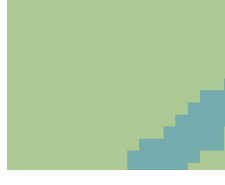
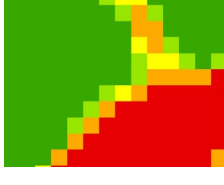
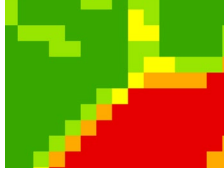
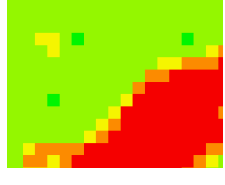
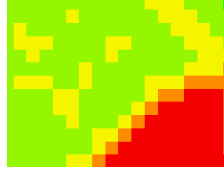
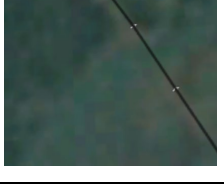


(c)

Figure 10 Hotspot Locations on (a) LST Map (2020) (b) NDVI Map (2020) (c) LULC Map (2015)

Table 5 Spatio-temporal analysis of hotspot regions of 1 to 4

Parameter (Mean Value)	1991	1998	2014	2020	Change from 1991 to 2020
<b>KINFRA INDUSTRIAL AREA</b>					
LST (°C)	 32.92	 33.80	 35.08	 35.46	2.54
NDVI	 0.37	 0.30	 0.24	 0.21	-0.16
Google Earth Image					
<b>CALICUT INTERNATIONAL AIRPORT AND KONDOTTY REGION</b>					
LST (°C)	 31.36	 32.01	 32.79	 33.32	1.96
NDVI	 0.29	 0.27	 0.24	 0.22	-0.07
Google Earth Image					

Parameter (Mean Value)	1991	1998	2014	2020	Change from 1991 to 2020
<b>PERINTALMANNA BUILT-UP AREA</b>					
LST (°C)	 31.62	 31.98	 33.22	 33.46	1.84
NDVI	 0.21	 0.20	 0.16	 0.15	-0.06
Google Earth Image					
<b>KADALUNDI BIRD SANCTUARY</b>					
LST (°C)	 29.88	 29.92	 30.26	 30.50	0.62
NDVI	 0.28	 0.25	 0.12	 0.10	-0.18
Google Earth Image					

**(a) Location 1 - KINFRA industrial area**

From the spatiotemporal analysis shown in Table 5, it is evident that the land use pattern changed. Initially, it was a vegetation-covered area, and hence it had a low temperature. In 1998 vegetation was replaced by barren land, and the temperature was seen to increase. In 2014 and 2020, the industrial area expanded and hence increased the anthropogenic heat generated from industrial activities, decreased vegetation, and increased built-up leading to the increase in temperature by 2.54°C.

**(b) Location 2 - Calicut International Airport and Kondotty region**

In the case of Calicut International Airport and Kondotty region (Table 5) from where the analysis has been derived, the dark paved surface and increased airport activities over time, with increased passenger load, mainly as it became an international airport, can be the reason for the high temperature. The airport is also attracting a considerable proportion of the population, who have occupied the area which was previously thick vegetation. In the case of the Kondotty region, decreased vegetation and increased built-up could be seen as the reasons for the increase in temperature over the years.

**(c) Location 3 - Perintalmanna built-up area**

In the Perintalmanna region (Table 5), the built-up area and the paved surfaces increased over time with decreased vegetation. It

is one of the regions with the highest increase in urban density and subsequently an LST increase of 1.84°C was observed. Increased anthropogenic activities in terms of vehicular emissions can also be a reason.

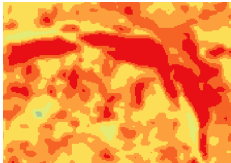
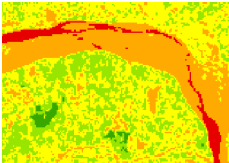
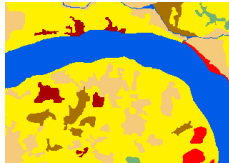
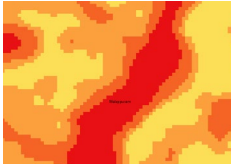
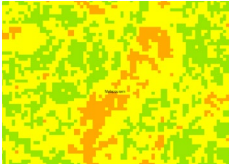
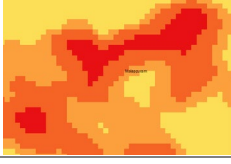
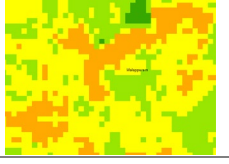
**(d) Location 4 - Kadalundi Bird Sanctuary**

In this region, in 1991, the temperature mean value is found to be 29.88°C and it increased to the range of 30.50°C in 2020, which is a slight increase of 0.62°C as mentioned in Table 5, hence a gradual increase in temperature over the years is evident which might affect the migratory birds in Kadalundi bird sanctuary. A decrease in vegetation intensity and an increase in built-up are seen in this area to be the reasons.

**(e) Location 5, 6, 7 – River sand, Fallow land, Barren land**

For the regions shown in Table 6, the sand is having a property of high heat fixation which could be the reason for the high temperature in that area. During the fallow period, the land surface albedo decreases and hence the reflectivity reduces and the temperature rises in the event of continued daylight exposure. As a result, the process of heat irradiation for the environment intensifies, mostly on a local scale (Kaiser et al., 2022).

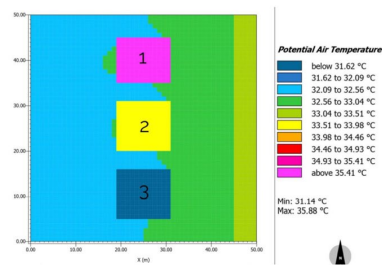
**Table 6** Hotspot locations 5, 6, 7: LST comparison with NDVI, Google Earth and Land Use

Location	LST	NDVI	Google Earth	Land Use
5. River sand (Bharathapuzha)				
6. Fallow land				
7. Barren land				

Through the spatiotemporal analysis of identified thermal hotspots based on remote sensing observations, it is evident that the increasing impact of urbanization and the subsequent change in land use patterns at the expense of greenery; and other anthropogenic factors have a significant effect on the local climate. The rising LST will have detrimental impacts on humans as well as the environment. An overall increase in surface temperature results in more frequent floods and other extreme weather events (Varughese & Purushothaman, 2021) as evident in the case of the 2018 and 2019 Kerala floods, where the Malappuram urban agglomeration region was considerably affected. Hence proper planning and enforcement of context-specific mitigation measures should be strictly performed.

## 5. Recommendations and Future Implications for UHI Mitigation

Seeing urbanization as a never-ending process, it is increasingly important to take the measures necessary to achieve a fine balance between the environment and urban expansion. As a result, activities should be performed to reduce heat gain. Accordingly, in the current study, two types of planning recommendations are put forward: 1) case-specific recommendations and 2) general planning recommendations.



### 5.1 Case-specific recommendations

The present section discusses the planning recommendations for the thermal hotspot locations as identified from the research work.

In the industrial region (location 1), where there are various sources of heat rejected from industrial processes, heat recovery can play a significant role, in reducing thermal pollution and decreasing the heat gain effect. For Perintalmanna built-up and Kondotty region (locations 2 and 3) and similar other regions, the use of cool or green roofs with urban farming can be encouraged. Increasing surface reflectivity using cool roofs, cool pavements and other high albedo building materials will help store less heat and maintain a low temperature. To validate this, an analysis using ENVIMET software was carried out (Yeo et al., 2021) and the air temperature difference between different roofing scenarios of identical one-story buildings was found as shown in Figure 11. The highest indoor temperature of 35.88°C was observed in RCC roofing. White-coated RCC roofing registered a temperature of 33.59°C. The lowest indoor air temperature of 31.14°C was observed on green roofs.

1. RCC roofing
2. White coated RCC roofing (Cool roofs)
3. Green roofs

Figure 11 Indoor Air temperature

The sand in fallow land (location 6) has got high heat fixation property, conversion to paddy or green areas can be carried out. Figure 12 maps the fallow land within the study area. The Kerala Conservation of Paddy Land and Wetland Act 2008 shall strictly be implemented. Also, the increased adoption of conservation tillage in agricultural areas can be suggested as it increases the surface albedo over that of the normal tilled cropland, which leads to a decrease in temperature. It reduces the frequency of equipment passages across the field, leading to reduced fuel consumption and the associated carbon emissions. It also increases the productivity of the cropland, improved water and fertilizer penetration and increased moisture levels in the soil. Local authorities need to plan awareness campaigns among the farmers and support systems to help farmers to adopt the conservation tillage practice.

Similar to fallow land, barren land (location 7) has also got high heat fixation properties, so strategies to convert to green zones

should be taken up. The area's existing open spaces are devoid of natural elements making them incapable of offering any connections with nature. Urban forestry serves as cooling "islands" in hot urban areas. They can also cool the surrounding landscape as per their scale and wind direction. As they provide cooling to areas downwind, they ought to be placed upwind of hotspot areas (Norton et al., 2013). In Melbourne, urban forestry is placed to the north of priority areas, as extreme heat occurrences are usually accompanied by high-pressure systems. East of Victoria, which bring warm continental air from the North. Royal Park for Melbourne's CBD is an example. Similar strategies may be applied in the case region as well. Since during summer wind flows from southwest to northeast along the study area, suitable vacant land locations are identified upwind of the hotspot regions as shown in Figure 13 where probable urban forestry can be carried out.

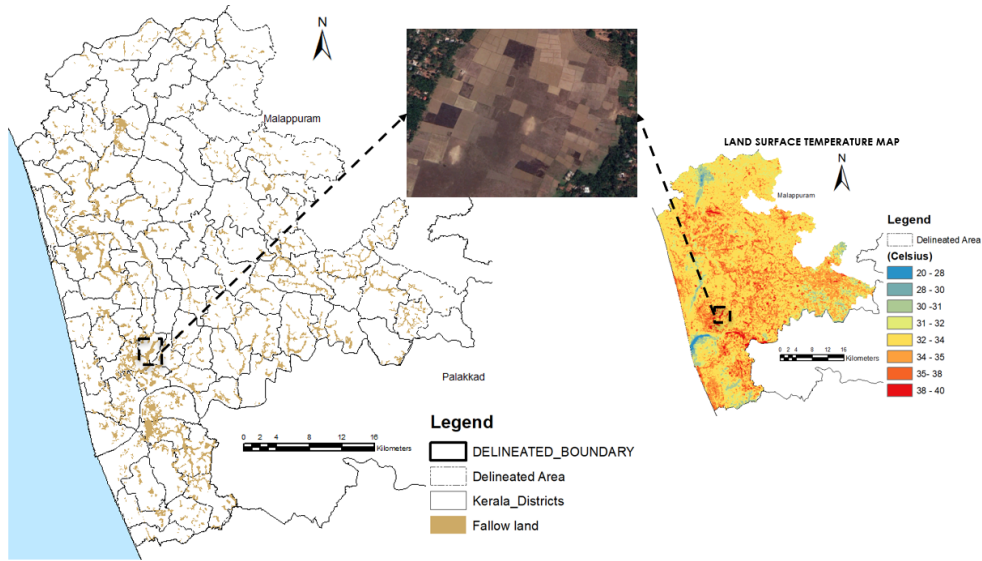


Figure 12 Reclamation of fallow land

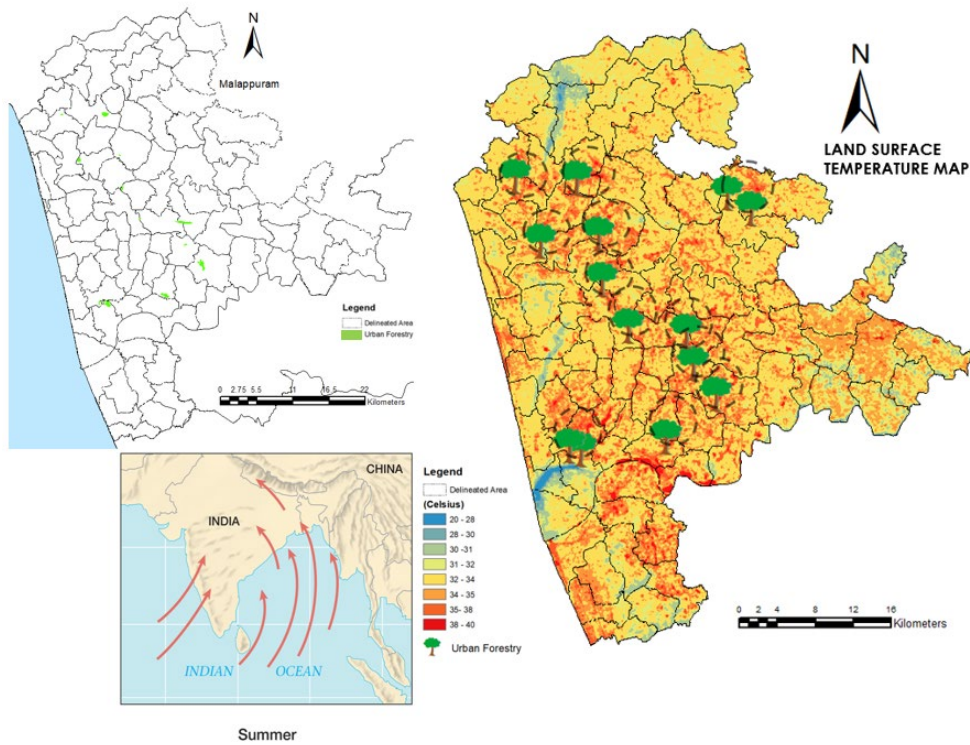
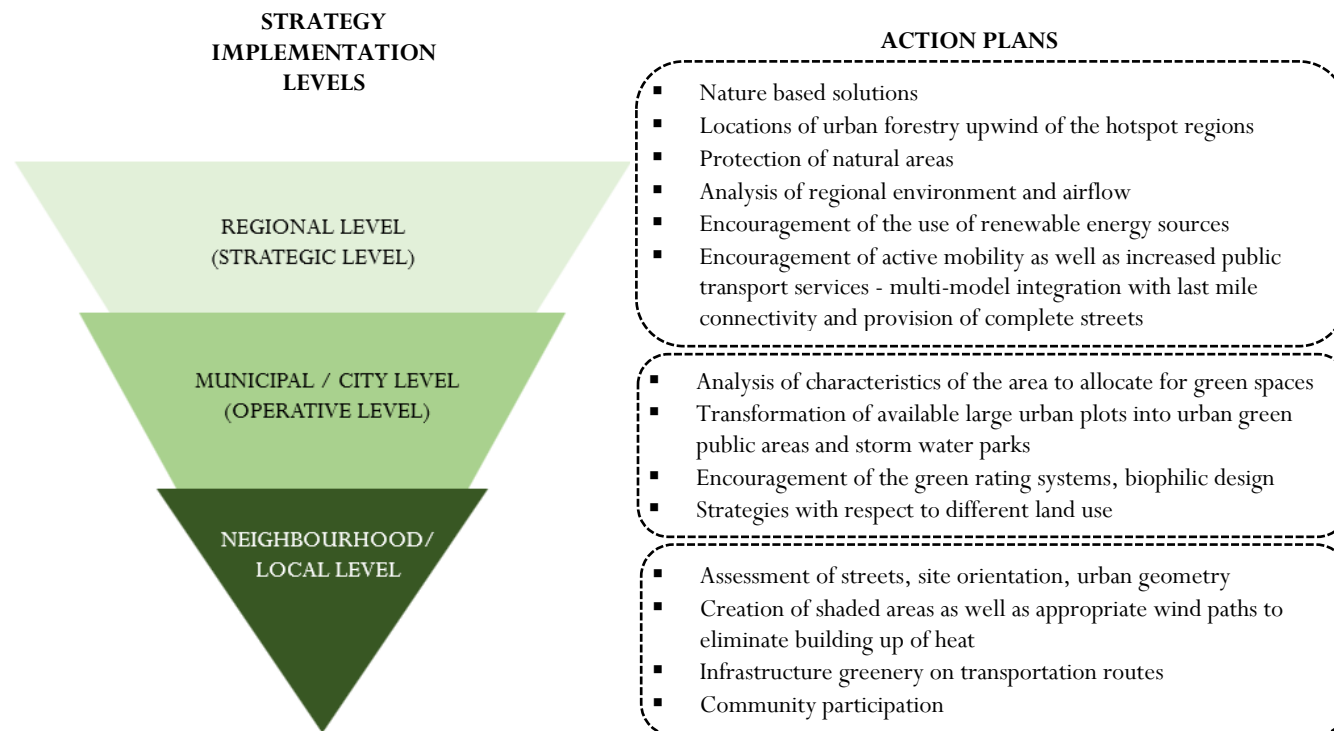


Figure 13 Barren land locations for urban forestry

### 5.2 General Planning Recommendations

The present section discusses some of the planning recommendations given based on the overall outcome of

the research work. They are explained in the subsequent paragraphs.



**Figure 14** Planning recommendations at various levels

Policies and cooperation at all scales are necessary for effective implementation, which can be improved through integrated solutions that connect mitigation and adaptation with other social goals. It is ideal to think of planning for strategies as a multi-level, hierarchical process (Figure 14). The regional level, which is a strategic level, is the first level. Various nature-based solutions can be incorporated. Suitable locations for urban forestry are to be selected upwind of the hotspot regions identified from this broad assessment. Agroforestry can also be promoted and the ecosystem for it needs to be created at the regional planning level. It is also important to encourage the preservation of vast natural regions, such as river basins contiguous to urban areas. Particularly, it is important to give natural areas like riparian zones and wetlands top priority for preservation so that stream buffers, sites for native plant regeneration, and storm-water parks can be created. Also, the use of renewable energy sources should be encouraged, and low-carbon fuels should be promoted. To reduce anthropogenic heat generation, encouragement of active mobility as well as increased public transport services with more comfort and convenience shall be implemented. Multi-model integration with last-mile connectivity helps in promoting these. Also, the creation of complete streets that provide a uniform carriageway, safe and continuous walkways, separated bike lanes, well-organized on-street parking and secured pedestrian crossings with refuge increases active mobility and should be taken up in the local area planning.

The shift from strategy to action occurs at the next level, which is the municipal or city level. To provide space for green areas,

the function and characteristics of the area should be examined. The creation of urban green public spaces like urban parks, urban forests, community gardens, etc. should be done by prioritizing existing large vacant urban plots that are available within the urban fabric. These spaces can be planned to include various environmental and recreational features as well as to boost urban biodiversity. Implementation of these nature-based solutions can be organized by municipalities, NGOs, etc. Encouragement of the green rating systems, where according to the rating certificate, the competent authority shall offer some incentives, for example, in terms of tax relaxation, can be provided to developers constructing housing, schools, resorts, etc. incorporating green infrastructure elements and tools and using sustainable means in creating the outdoor landscape. The incorporation of various green infrastructure components into new building designs may be required by new regulations, which will both serve to improve the environment and the building's internal efficiency. Commercial buildings can plant trees in parking lots and around buildings, green walls and green facades in areas with less ground space. Residential buildings shall have trees around as well as rooftop farming can be carried out. Biophilic design can be incorporated that seeks to connect people with nature and natural elements. Integrating living greenery, use of natural materials and water features, encouraging natural ventilation and incorporating atriums or courtyards with vegetation, use of natural shading devices such as awnings, trellises, pergolas, etc can be used. It results in significant reductions in the amount of energy usage as it reduces the dependency on cooling appliances. Green pavements can also be

adopted. By incorporating these biophilic design elements, spaces become more than just functional structures - they become vibrant and inspiring environments that reconnect people with nature. These design strategies promote well-being, improve air quality, regulate temperature, reduce energy consumption, and enhance the overall human experience within the built environment (Browning et al., 2014).

Next is the neighbourhood/ local level, where the assessment of streets and site orientation, land slopes, vacant sites, community participation, etc. are carried out for creating green spaces. Infrastructure greenery on transportation routes can be given, where existing infrastructure, such as tunnels, bridges, motorways, and bus stops, can be enhanced by vegetation to reduce the impact of dark pavements on heat gain. Urban geometry also plays a role in controlling heat gain. The coverage of the shaded areas along with the wind condition is influenced by building layout, the placement of urban features, building proportion and orientation. Additionally, sufficient urban planning is essential at a coarser spatial scale to take advantage of the regional environment and airflow, create appropriate wind paths that access the urban area, and eliminate the building up of heat. When planning new construction or a building retrofit, the height of the buildings ideally should be in ascending order to the wind direction so that sufficient wind can enter the rear blocks. To improve airflow, staggering building heights and void decks would also be an option. Ventilation into a building and on the streets can be influenced by the building form and composition. Pilot projects to create awareness regarding the benefits should be carried out. Programs can begin as voluntary initiatives and then expand to building codes as heat gain adaptation measures and norms. It is recommended that local governments use as many effective mitigation measures and technologies as they can for their municipal buildings and facilities, thereby leading as an example for private buildings. To showcase the cost-effectiveness, energy savings, and other advantages of these approaches, cities should document their experiences with them. Local governments should take up the initiative and provide awareness to the people through effective implementation.

## 6 Conclusions

The present study conducted for Malappuram urban agglomeration area in Kerala, India, revealed that similar to other metropolitan areas in the country, it showed a major rise in the land surface temperature, a 1.70°C rise was seen over 30 years from 1991 to 2020. A significant decrease in the maximum value of NDVI from 0.90 to 0.60 was also observed, which indicates that the vegetation intensity is decreasing. Hence various tree planting strategies within the urban areas, with local, micro and macro scale forestry are to be looked into to combat the reduction in vegetation cover along with the other strategies suggested. Areas with the highest increase in urban density with decreased vegetation observed an LST increase of around 1.84°C. This could be attributed possibly to the minor impacts of climate change as well as the loss of green cover as evident from the LULC and NDVI maps.

The current research focuses only on the broader level of assessment as the study was carried out with the help of remote

sensing satellite data since it covered a larger region. Hence, this study can be taken as the first level of assessment by finding the areas to focus on for further analysis which can be carried out using more sophisticated tools like an aircraft thermal scanner, infrared thermometer, etc. which provides better resolution and details. The identified thermal hotspots and similar regions should be further analyzed to give appropriate context-specific mitigation strategies. Model simulations using various software like ENVIMET can be carried out to analyze the microclimate using different planning scenarios and suggest measures through Development Control Regulations. The urban geometry, FAR (Floor Area Ratio), the orientation of buildings, green cover, type of roofing, etc. could be varied in different scenarios and suitable economical and context-specific measures can be implemented to reduce the heat gain (Yeo et al., 2021). Further, the planning recommendations and the mitigation strategies proposed need to be verified or validated by the policymakers or planners.

Proper effective planning is required to subside the effect on the local climate due to the increasing impact of urbanization and the subsequent change in land use patterns at the expense of greenery. Policy recommendations must include consideration of the urban thermal landscape and proper mitigative measures should be taken up; obliviousness of it will have a harmful effect on the environment, meteorology, daily life and health.

## Acknowledgements

The authors express their gratitude to the reviewers whose valuable input significantly enhanced the quality of this manuscript. The authors would also like to acknowledge National Institute of Technology, Calicut for the support in carrying out this study.

## References

- Aik, J., Ismail, M. H., & Muharam, F. M. (2020). Land Use / Land Cover Changes and the Relationship. *Land*, 9(372): 1–23.
- Avdan, U., & Jovanovska, G. (2016). Algorithm for Automated Mapping of Land Surface Temperature Using LANDSAT 8 Satellite Data. *Journal of Sensors*, 2016: 8, Article ID 1480307. <https://doi.org/10.1155/2016/1480307>
- Banerji, H., Firoz, M., & Sen, J. (2014). A Methodology to Define the Typology of Rural Urban Continuum Settlements in Kerala. *Journal of Regional Development and Planning*, 3(1), 49.
- Bhuvan. (2021). *Thematic Data dissemination*. Bhuvan ISRO/ NRSC. <https://bhuvan-app1.nrsc.gov.in/thematic/thematic/index.php> Retrieved September 14, 2021
- Browne, D. (2019). Leaving no one behind. *Highways*, 88(5): 3. <https://doi.org/10.4324/9781351006941-3>
- Browning, W., Ryan, C., & Clancy, J. (2014). 14 Patterns of Biophilic Design: Improving Health & Well-Being in the Built Environment. *Terrapin Bright Green, LLC*, 1–60. <https://doi.org/10.1016/j.yebh.2008.04.024>
- Business Standard News. (2022). *90 people died in 2022 due to heatwave spells in India, Pakistan: Study*. <https://www.business-standard.com/article/current-affairs/90-people-died-in-2022-due-to->

- heatwave-spells-in-india-pakistan-study-122052400052\_1.html (Retrieved October 24, 2022)
- Carbon Management Ask the Experts: *The IPCC Fifth Assessment Report*. (2014). <https://doi.org/10.4155/cmt.13.80>
- Carlson, T. N., & Ripley, D. A. (1997). On the relation between NDVI, fractional vegetation cover, and leaf area index. *Remote Sensing of Environment*, 62(3): 241–252. [https://doi.org/10.1016/S0034-4257\(97\)00104-1](https://doi.org/10.1016/S0034-4257(97)00104-1)
- Chen, J., & Zhang, L. (2016). Joint multi-image saliency analysis for region of interest detection in optical multispectral remote sensing images. *Remote Sensing*, 8(6): 461. <https://doi.org/10.3390/rs8060461>
- Cheval, S., & Dumitrescu, A. (2009). The July urban heat island of Bucharest as derived from modis images. *Theoretical and Applied Climatology*, 96(1–2): 145–153. <https://doi.org/10.1007/S00704-008-0019-3>
- Cyriac, S., & Firoz C, M. (2022). Dichotomous classification and implications in spatial planning: A case of the Rural-Urban Continuum settlements of Kerala, India. *Land Use Policy*, 114: 105992. <https://doi.org/https://doi.org/10.1016/j.landusepol.2022.105992>
- Deng, C., & Wu, C. (2013). Examining the impacts of urban biophysical compositions on surface urban heat island: A spectral unmixing and thermal mixing approach. *Remote Sensing of Environment*, 131: 262–274. <https://doi.org/10.1016/J.RSE.2012.12.020>
- Estoque, R. C., & Murayama, Y. (2017). Monitoring surface urban heat island formation in a tropical mountain city using Landsat data (1987–2015). *ISPRS Journal of Photogrammetry and Remote Sensing*, 133: 18–29. <https://doi.org/10.1016/j.isprsjprs.2017.09.008>
- Fathima Zehba, M. P., Mohammed Firoz, C., & Babu, N. (2021). Spatial Assessment of Quality of Life Using Composite Index. *Quality of Life*, 181–207. <https://doi.org/10.1201/9781003009139-11>
- Feizizadeh, B., Blaschke, T., Nazmfar, H., Akbari, E., & Kohbanani, H. R. (2013). Monitoring land surface temperature relationship to land use/land cover from satellite imagery in Maraqeh County, Iran. <http://Dx.Doi.Org/10.1080/09640568.2012.717888>, 56(9): 1290–1315. <https://doi.org/10.1080/09640568.2012.717888>
- Gazi, M. Y., Rahman, M. Z., Uddin, M. M., & Rahman, F. M. A. (2021). Spatio-temporal dynamic land cover changes and their impacts on the urban thermal environment in the Chittagong metropolitan area, Bangladesh. *GeoJournal*, 86(5): 2119–2134. <https://doi.org/10.1007/s10708-020-10178-4>
- Gohain, K. J., Mohammad, P., & Goswami, A. (2021). Assessing the impact of land use land cover changes on land surface temperature over Pune city, India. *Quaternary International*, 575–576: 259–269. <https://doi.org/10.1016/j.quaint.2020.04.052>
- Grover, A., & Singh, R. B. (2015). Analysis of urban heat island (Uhi) in relation to normalized difference vegetation index (ndvi): A comparative study of delhi and mumbai. *Environments - MDPI*, 2(2): 125–138. <https://doi.org/10.3390/environments2020125>
- Grover, A., & Singh, R. B. (2016). Monitoring Spatial patterns of land surface temperature and urban heat island for sustainable megacity: A case study of Mumbai, India, using landsat TM data. *Environment and Urbanization ASIA*, 7(1): 38–54. <https://doi.org/10.1177/0975425315619722>
- Guha, S., & Govil, H. (2020). Land surface temperature and normalized difference vegetation index relationship: a seasonal study on a tropical city. *SN Applied Sciences*, 2(10): 1–14. <https://doi.org/10.1007/s42452-020-03458-8>
- Haghighi, N., Liu, X. C., Zhang, G., & Porter, R. J. (2018). Impact of roadway geometric features on crash severity on rural two-lane highways. *Accident Analysis and Prevention*, 111(November 2017): 34–42. <https://doi.org/10.1016/j.aap.2017.11.014>
- Hu, L., & Brunsell, N. A. (2013). The impact of temporal aggregation of land surface temperature data for surface urban heat island (SUHI) monitoring. *Remote Sensing of Environment*, 134: 162–174. <https://doi.org/10.1016/j.rse.2013.02.022>
- Kafy, A. Al, Faisal, A. Al, Shuvo, R. M., Naim, M. N. H., Sikdar, M. S., Chowdhury, R. R., Islam, M. A., Sarker, M. H. S., Khan, M. H. H., & Kona, M. A. (2021). Remote sensing approach to simulate the land use/land cover and seasonal land surface temperature change using machine learning algorithms in a fastest-growing megacity of Bangladesh. *Remote Sensing Applications: Society and Environment*, 21(December 2020): 100463. <https://doi.org/10.1016/j.rsase.2020.100463>
- Kaiser, E. A., Beatriz, S., Rolim, A., Efrain, A., Grondona, B., Hackmann, C. L., Linn, R. D. M., Käfer, P. S., & Souza, N. (2022). Spatiotemporal Influences of LULC Changes on Land Surface Temperature in Rapid Urbanization Area by Using Landsat-TM and TIRS Images. *Atmosphere*, 13(3):460.
- Kallingal, F. R., & Joy, K. P. (2022). Regional Integrated Approach for Smart Master Planning: A Case of Kochi, Kerala, India. *Advances in 21st Century Human Settlements*, 231–247. [https://doi.org/10.1007/978-981-19-2386-9\\_6](https://doi.org/10.1007/978-981-19-2386-9_6)
- Kallingal, F. R., & Mohammed Firoz, C. (2022). Regional disparities in social development: A case of selected districts in Kerala, India. *GeoJournal*, 88: 1–28. <https://doi.org/10.1007/s10708-022-10592-w>
- Kikon, N., Singh, P., Singh, S. K., & Vyas, A. (2016). Assessment of urban heat islands (UHI) of Noida City, India using multi-temporal satellite data. *Sustainable Cities and Society*, 22: 19–28. <https://doi.org/10.1016/j.scs.2016.01.005>
- Madanian, M., Soffianian, A. R., Soltani Koupai, S., Pourmanafi, S., & Momeni, M. (2018). The study of thermal pattern changes using Landsat-derived land surface temperature in the central part of Isfahan province. *Sustainable Cities and Society*, 39: 650–661. <https://doi.org/10.1016/j.scs.2018.03.018>
- Mathew, A., Sreekumar, S., Khandelwal, S., Kaul, N., & Kumar, R. (2016). Prediction of surface temperatures for the assessment of urban heat island effect over Ahmedabad city using linear time series model. *Energy and Buildings*, 128: 605–616. <https://doi.org/10.1016/j.enbuild.2016.07.004>
- Ministry of Housing and Urban Affairs. (2017). *National Capital Region Planning Board*. <https://ncrpb.nic.in/rationale.html> (Retrieved November 20, 2022)
- National Remote Sensing Agency. (2007). *Natural Resources Census National Land Use and Land Cover Mapping Using Multi-Temporal AWiFS Data*. June.
- Norton, B., Bosomworth, K., Coutts, A., Williams, N., Livesley, S., Trundle, A., Harris, R., & Mcevoy, D. (2013). *Planning for a Cooler Future : Green Infrastructure to Reduce Urban Heat: Climate Adaptation for*

- Decision-makers. October, 1–29. [http://www.vcccar.org.au/sites/default/files/publications/VCCCAR\\_Green\\_Infrastructure\\_Guide\\_Final.pdf](http://www.vcccar.org.au/sites/default/files/publications/VCCCAR_Green_Infrastructure_Guide_Final.pdf)
- Praveen Lal, C. S., & Nair, S. B. (2017). Urbanization in Kerala—What Does the Census Data Reveal? *Indian Journal of Human Development*, 11(3): 356–386. <https://doi.org/10.1177/0973703018763241>
- Revi, A., Satterthwaite, D., Aragón-Durand, F., Corfee-Morlot, Robert B R Kiunsi, J., Pelling, M., Roberts, D., Solecki, W., Pahwa, S., & Sverdlík, A. (2014). Towards transformative adaptation in cities: the IPCC's Fifth Assessment. *IIED*, 26(1): 11–28. <https://doi.org/10.1177/0956247814523539>
- Rimal, B. (2012). Urbanization and the Decline of Agricultural Land in Pokhara Sub-metropolitan City, Nepal. *Journal of Agricultural Science*, 5(1): 54–65. <https://doi.org/10.5539/jas.v5n1p54>
- Rosenzweig, C.; Solecki, W.D.; Romero-Lankao, P.; Mehrotra, S.; Dhakal, S.; Ibrahim, S. A. (2018). Climate Change and Cities: Second Assessment Report of the Urban Climate Change Research Network. Cambridge University Press: Cambridge, UK. <https://doi.org/10.1080/23298758.1994.10685604>
- Ruefenacht, L. A., & Acero, J. A. (2017). Strategies for Cooling Singapore. *Cooling Singapore (CS), 2017*. <https://doi.org/10.3929/ethz-b-000258216>
- Sannigrahi, S., Rahmat, S., Chakraborti, S., Bhatt, S., & Jha, S. (2017). Changing dynamics of urban biophysical composition and its impact on urban heat island intensity and thermal characteristics: the case of Hyderabad City, India. *Modeling Earth Systems and Environment*, 3(2): 647–667. <https://doi.org/10.1007/s40808-017-0324-x>
- Sattari, F., & Hashim, M. (2014). A Brief Review of Land Surface Temperature Retrieval Methods from Thermal Satellite Sensors. *Middle-East Journal of Scientific Research*, 22(5): 757–768. <https://doi.org/10.5829/idosi.mejsr.2014.22.05.21934>
- Sekertekin, A., & Bonafoni, S. (2020). Land surface temperature retrieval from Landsat 5, 7, and 8 over rural areas: Assessment of different retrieval algorithms and emissivity models and toolbox implementation. *Remote Sensing* 12(2): 294. <https://doi.org/10.3390/rs12020294>
- Sholihah, R. I., & Shibata, S. (2019). Retrieving Spatial Variation of Land Surface Temperature Based on Landsat OLI/TIRS: A Case of Southern part of Jember, Java, Indonesia. *IOP Conference Series: Earth and Environmental Science*, 362(1). <https://doi.org/10.1088/1755-1315/362/1/012125>
- Singh, P., Kikon, N., & Verma, P. (2017). Impact of land use change and urbanization on urban heat island in Lucknow city, Central India. A remote sensing based estimate. *Sustainable Cities and Society*, 32, 100–114. <https://doi.org/10.1016/j.scs.2017.02.018>
- Singh, R. B., Grover, A., & Zhan, J. (2014). Inter-seasonal variations of surface temperature in the urbanized environment of Delhi using landsat thermal data. *Energies*, 7(3), 1811–1828. <https://doi.org/10.3390/en7031811>
- Skymet Weather Services. (2016). *Some more days of heatwave in Kerala before brief respite*. <https://www.skymetweather.com/content/weather-news-and-analysis/kerala-records-highest-temperature-in-almost-3-decades/> (Retrieved January 08, 2022)
- Sobrino, J. A., Jiménez-Muñoz, J. C., & Paolini, L. (2004). Land surface temperature retrieval from LANDSAT TM 5. *Remote Sensing of Environment*, 90(4): 434–440. <https://doi.org/10.1016/j.rse.2004.02.003>
- Sreenath, G. (2013). *Ground Water Information Booklet of Malappuram District*. December, 1–29.
- Sruthi Krishnan, V., & Mohammed Firoz, C. (2020). Regional urban environmental quality assessment and spatial analysis. *Journal of Urban Management*, 9(2): 191–204. <https://doi.org/10.1016/j.jum.2020.03.001>
- Sterling, S., & Duchame, A. (2008). Comprehensive data set of global land cover change for land surface model applications. *Global Biogeochemical Cycles*, 22(3): GB3017. <https://doi.org/10.1029/2007GB002959>
- T.S., S., Mohammed Firoz, C., & Bhagyanathan, A. (2022). The impact of upstream land use land cover change on downstream flooding: A case of Kuttanad and Meenachil River Basin, Kerala, India. *Urban Climate*, 41(April 2021): 101089. <https://doi.org/10.1016/j.uclim.2022.101089>
- The Hindu. (2019). *Sunstroke claims three lives in Kerala*. <https://www.thehindu.com/news/national/kerala/two-more-suspected-sunstroke-deaths/article26627812.ece> (Retrieved October 18, 2021)
- Tran, D. X., Pla, F., Latorre-Carmona, P., Myint, S. W., Caetano, M., & Kieu, H. V. (2017). Characterizing the relationship between land use land cover change and land surface temperature. *ISPRS Journal of Photogrammetry and Remote Sensing*, 124: 119–132. <https://doi.org/10.1016/j.isprsjprs.2017.01.001>
- Twumasi, Y. A., Merem, E. C., Namwamba, J. B., Mwakimi, O. S., Ayala-Silva, T., Frimpong, D. B., Ning, Z. H., Asare-Ansah, A. B., Annan, J. B., Oppong, J., Loh, P. M., Owusu, F., Jeruto, V., Petja, B. M., Okwemba, R., McClendon-Peralta, J., Akinrinwoye, C. O., & Mosby, H. J. (2021). Estimation of Land Surface Temperature from Landsat-8 OLI Thermal Infrared Satellite Data. A Comparative Analysis of Two Cities in Ghana. *Advances in Remote Sensing*, 10(04): 131–149. <https://doi.org/10.4236/ars.2021.104009>
- United Nations. (2019). *The Climate Crisis – A Race We Can Win | United Nations*. <https://www.un.org/en/un75/climate-crisis-race-we-can-win> (Retrieved December 30, 2021)
- United States Geological Survey. (2022). *EarthExplorer*. <https://earthexplorer.usgs.gov/> (Retrieved August 10, 2021)
- Vancutsem, C., Ceccato, P., Dinku, T., & Connor, S. J. (2010). Evaluation of MODIS land surface temperature data to estimate air temperature in different ecosystems over Africa. *Remote Sensing of Environment*, 114(2): 449–465. <https://doi.org/10.1016/j.rse.2009.10.002>
- Varughese, A., & Purushothaman, C. (2021). Climate Change and Public Health in India: The 2018 Kerala Floods. *World Medical and Health Policy*, 13(1), 16–35. <https://doi.org/10.1002/wmh3.429>. *World Medical and Health Policy*, 13(1): 16–35. <https://doi.org/10.1002/wmh3.429>
- Voogt, J. A., & Oke, T. R. (2003). Thermal remote sensing of urban climates. *Remote Sensing of Environment*, 86(3): 370–384. [https://doi.org/10.1016/S0034-4257\(03\)00079-8](https://doi.org/10.1016/S0034-4257(03)00079-8)

Weng, Q., & Fu, P. (2014). Modeling diurnal land temperature cycles over Los Angeles using downscaled GOES imagery. *ISPRS Journal of Photogrammetry and Remote Sensing*, 97: 78–88. <https://doi.org/10.1016/j.isprsjprs.2014.08.009>

Wilson, J. S., Clay, M., Martin, E., Stuckey, D., & Vedder-Risch, K. (2003). Evaluating environmental influences of zoning in urban ecosystems with remote sensing. *Remote Sensing of Environment*, 86(3): 303–321. [https://doi.org/10.1016/S0034-4257\(03\)00084-1](https://doi.org/10.1016/S0034-4257(03)00084-1)

World Health Organisation. (2022). *Heatwaves*. [https://www.who.int/health-topics/heatwaves#tab=tab\\_1](https://www.who.int/health-topics/heatwaves#tab=tab_1)

Yeo, L. B., Hoh, G., Ling, T., & Tan, M. L. (2021). Interrelationships between Land Use Land Cover (LULC) and Human Thermal Comfort (HTC): A Comparative Analysis of Different Spatial Settings, *Sustainability*, 13(1): 382. <https://doi.org/10.3390/su13010382>

Zullo, F., Fazio, G., Romano, B., Marucci, A., & Fiorini, L. (2019). Effects of urban growth spatial pattern (UGSP) on the land surface temperature (LST): A study in the Po Valley (Italy). *Science of The Total Environment*, 650: 1740–1751. <https://doi.org/10.1016/j.scitotenv.2018.09.331>